King Saud University

Arabian Journal of Chemistry

www.ksu.edu.sa
www.sciencedirect.com

ORIGINAL ARTICLE

Anti-human colon cancer properties of a novel chemotherapeutic supplement formulated by gold nanoparticles containing *Allium sativum* L. leaf aqueous extract and investigation of its cytotoxicity and antioxidant activities

Qingbin Liu [a], Fenglian Wu [b], Yanxin Chen [c,*], Sara T. Alrashood [d], Sulaiman Ali Alharbi [e]

[a] *Department of General Surgery, The First Hospital of Qin Huangdao, Qinhuangdao 066000, China*
[b] *Department of Plastic Surgery, The First Hospital of Qin Huangdao, Qinhuangdao 066000, China*
[c] *Department of Pathology, The First Hospital of Qin Huangdao, Qinhuangdao 066000, China*
[d] *Department of Pharmaceutical Chemistry, College of Pharmacy, King Saud University, Riyadh 11451, Saudi Arabia*
[e] *Department of Botany and Microbiology, College of Science, King Saud University, PO Box 2455, Riyadh 11451, Saudi Arabia*

Abstract   Recently, scientists have tried to increase organic chemistry productions for the treatment of many cancers such as colon cancers. Au nanoparticles have a special role in the treatment of several cancers. Furthermore, one of the therapeutic properties of *Allium sativum* L. is increasing the physiological potentials of the body against different cancers. In the current research, gold nanoparticles were prepared and synthesized in aqueous medium using *Allium sativum* L. leaf extract. Also, we investigated the anti-colon cancers potentials of these nanoparticles against colon cancer cell lines. The FT-IR, UV–Vis, FE-SEM, and TEM tests used to determine the physiochemical properties of the recent nanoparticles. The results of FE-SEM and TEM images indicated the average size of 19 nm. DPPH test was carried out to assess the antioxidant capacities of $HAuCl_4$, *A. sativum*, and AuNPs. DPPH test revealed similar antioxidant potentials for *A. sativum*, AuNPs and butylated hydroxytoluene. For the determining of anti-colon cancer properties of $HAuCl_4$, *A. sativum*, and AuNPs, MTT assay was used on HUVECs (Normal), HT-29 (Colorectal adenocarcinoma), HCT 116 (Colorectal carcinoma), HCT-8 [HRT-18] (Ileocecal colorectal

* Corresponding author.
  E-mail address: chenyanxin76@sina.com (Y. Chen).
Peer review under responsibility of King Saud University.

ELSEVIER   **Production and hosting by Elsevier**

adenocarcinoma), and Ramos.2G6.4C10 (Burkitt's lymphoma) cell lines. AuNPs had very low cell viability and anti-colon cancer effects dose-dependently against HT-29, HCT 116, HCT-8 [HRT-18], and Ramos.2G6.4C10 cell lines. The best result of anti-colon cancer activities of AuNPs against above cell lines was observed in the case of the HCT 116 cell line. In conclusion, the synthesized AuNPs revealed remarkable anti-colon cancer properties against colon cell lines. It seems the above nanocomposite can be used as a novel chemotherapeutic material in the future.

1. Introduction

Colon is the last part of the gastrointestinal system that participates in the water and partially food absorption. The normal function of the colon is necessary for the routine activities of the body (Juul et al., 2018). The major diseases that influence the usual function of the colon are included colon cancer, crohn's disease, lactose intolerance, inflammatory bowel disease, diarrhea, appendicitis, acid reflux (GERD), hemorrhoids, gallstones, celiac disease, irritable bowel syndrome, listeria infection, stomach ulcers, tapeworms, and ulcerative colitis. Colon cancer or colorectal cancer is one of the most common cancers in both developing and developed countries. In first, colon cancer appears in the form of the polyp and after a while it spreads in all parts of the colon (Astin et al., 2011). The signs of colon cancer are loss of appetite, worsening constipation, feeling tired all the time, nausea or vomiting, change in bowel movements, decrease in stool caliber, blood in the stool, rectal bleeding or anemia, and weight loss (Juul et al., 2018; Astin et al., 2011). The main risk factors of colon cancer are radiation therapy, sedentary lifestyle, inherited syndromes, African-American race, alcohol, high-fat diet, inflammatory intestinal conditions, older age, smoking, family history of colon cancer, obesity, diabetes, and personal history of polyps (Juul et al., 2018; Astin et al., 2011). Medical imaging such as positron-emission tomography, computerized tomography scan, and MRI, histopathology, and staging are used to diagnosis the colon cancer (Cunningham et al., 2010). The main lifestyle changes that reduce the rate of colon cancer are included maintain a healthy weight, stop smoking, eat a variety of vegetables, fruits, and whole grains, and exercise most days of the week (Lauby-Secretan et al., 2016). For the treatment of colon cancer, chemotherapy, radiation therapy, and immunotherapy are used. The major anti-colon cancer chemotherapeutic materials are included panitumumab, cetuximab, fluorouracil, irinotecan, and oxaliplatin (Shaib et al., 2013). Due to the severe side effects of chemotherapy, the scientists have tried to formulate other drugs by metallic nanoparticles (Zangeneh and Zangeneh, 2019; Hemmati et al., 2019).

Nanobiotechnology is a combination of nanotechnology and biotechnology and has a remarkable role in the development and application of many useful tools and technologies in life science-related research (Raut et al., 2010; Varma, 2012). In the past decade, nanobiotechnology has come to the fore as a science that has led to reform changes in medicines (Varma, 2012). Nanomaterials, which are the subject of our study, have unique competencies different from their macro-scale counterparts due to their low volume/surface ratio and many advanced and new physiochemical properties such as color, solubility, strength, prevalence, toxicity, magnetic, optical, thermodynamics (Arunachalam et al., 2003; Sintubin et al., 2009). In recent years, biological methods that non-toxic, cost-effective, and environmentally friendly have become the focus of interest compared to physicochemical nanoparticle synthesis methods (Arunachalam et al., 2003; Sintubin et al., 2009; Ball, 2018). Various pathways have been developed for the biogenic or biological formulation of nanomaterials from the salts of different metal ions. The synthesis of nanoparticles under purely 'green' principles can be achieved by using an environmentally compatible solvent system with environmentally friendly stabilizing and reducing factors (Zangeneh, 2019; Mohammadi et al., 2019; Zangeneh et al., 2019). The basic principle in the biogenesis of nanoparticles is the reduction of metal ions of several biomolecules found in organisms. In addition to reducing the environmental impact of biological synthesis, it enables the production of large quantities of nanoparticles, which are well defined in size and morphology, independent of contamination. Microorganisms, marine algae, plant extracts, plant tissue, fruits, and all plants are administrated to formulate nanomaterials (Mahdavi et al., 2019; Ahmeda et al., 2020; Ghaneialvar et al., 2019; Goorani et al., 2020). The reduction of metal ions using plant extracts has been a known method since the 1900s. Due to the poor understanding of the mechanisms of the reducing agents, it has increased interest in the past 30 years. Recently, scientists have revealed that medicinal plants' green synthesized-metallic nanoparticles have excellent anti-cancer properties. Metallic nanoparticles have achieved notable consideration in the field of medicine (Goorani et al., 2019; Jalalvand et al., 2019; Moradi et al., 2019). Some studies conducted today have shown that some nanoparticles have therapeutic properties and it is an excellent alternative to physicochemically different metal-supported nanoparticles, antibacterial, and especially anticancer drugs (Rashidi et al., 2018; Sherkatolabbasieh et al., 2017; Zhaleh et al., 2018).

Gold nanoparticles have attracted attention among all other nanoparticles due to their wide use in optical, electrical, chemical, sensor, and biological improvement and fields (Zhaleh et al., 2019; Tahvilian et al., 2019). They have been synthesized due to the anti-cancer, antioxidant, antifungal, anti-parasitic, and antibacterial properties (Singh et al., 2018). Among the above remedial properties, the anticancer potentials are important. In previous studies, it showed excellent anticancer potentials against various cell lines of gold nanoparticles such as Lewis lung carcinoma (LL2) cells, ADR/MCF-7 cancer cells, A549 lung epithelial cancer cell line, HT29, HCT15, HCT116, and RKO colon cancer cell lines, U87 and LN229 human glioma cancer lines, A549 cells and HeLa cells, HepG2-R, HDF, and C0045C, 4T1 mouse mammary carcinoma cell line, A549, H460, and H520 human lung

cancer cells (Zhaleh et al., 2019; Tahvilian et al., 2019; Singh et al., 2018). So far, any study hasn't been done about the remedial capacities of natural compounds green-synthesized Au nanoparticles in the treatment of colon cancers.

In recent years, researchers have applied the anticancer effects of ethno medicinal herbs for synthesizing the gold nanocomposite. The anticancer activities of *Lubinus perennis*, *Solanum seaforthianum*, *Tinospora cordifolia*, *Sophora subprostrata*, *Euphoria hirta*, *Maytenus boaria*, *Cephaelis acuminate*, *Phyllanthus niruri*, *Boswellia serrate*, *Barleria prionitis*, *Lavendula officinalis*, and *Cephalotaxus harringtonia* drupacea have been proved (Soni and Krishnamurthy, 2013). In traditional medicine, people use the *Allium sativum* L. for the prevention, control, and cure of various cancers such as breast, prostate, ovarian, and blood cancers (Thomson and Ali, 2003). The main antioxidant and anticancer compounds of *A. sativum* are diallyl thiosulfinate, diallyl tetrasulfide, methyl allyl trisulfide, dipropyl sulfide, dially trisulfide, S-allyl cysteine sulfoxide, allyl methane sulfinate, diallyl disulfide, 3-vinyl-4H-1,2-dithiin, allyl methyl thiosulfinate, S-methyl cysteinesulfoxide, dipropyldi sulfide, dimethyl disulfide, 3-vinyl-6H-1,2-dithiin, methyl-propyl disulfide, S-propyl cysteine sulfoxide, dimethyl sulfide, methyl methane sulfinate, and 3-vinyl-6H-1,3-dithiin (Thomson and Ali, 2003).

Accordingly, the present experiment was conducted to evaluate the possible anti-colon cancer activity of synthesized gold nanoparticles using *A. sativum* leaf aqueous extract against common cell lines of colon cancer included HCT-8 [HRT-18], HCT 116, HT-29, and Ramos.2G6.4C10.

2. Materials and methods

2.1. Material

Bovine serum, 2,2-diphenyl-1- pikrilhydrazil (DPPH), dimethyl sulfoxide (DMSO), decamplmaneh fetal, 4-(Dimethylamino) benzaldehyde, hydrolyzate, antimycotic antibiotic solution, Ehrlich solution, and borax-sulfuric acid mixture, DMED, all were afforded from the US Sigma-Aldrich company.

2.2. Synthesis of AuNPs

To obtain the aqueous extract of the plant, 250 gr of the dried branches of the *A. sativum* leaves were poured in a container containing 2000 mL boiled water, and the container lid was tightly closed for 4 h. Then, the content of the container was filtered, and the remaining liquid was placed on a bain-marie to evaporate. Finally, a tar-like material was obtained, which was powdered by a freeze dryer.

The extract of the *A. sativum* leaves was prepared for the green synthesis method was extracted with distilled water in the microwave. Green synthesis of gold nanoparticles was started with such a process combination of 100 mL HAuCl₄·H₂O at concentrations of 10^{-3} M and 400 mL of *A. sativum* leaf aqueous isolate (20 µg / mL) in a cylindrical flask.

The reaction mixture was kept under magnetic stirring for 12 h at room temperature. At the end of the reaction time, the dark yellow colored colloidal solution of Au was formed. The solution was centrifuged at 10,000 rpm for 15 min. The precipitate was sprayed with water and then resuspended (Hemmati et al., 2019).

Various analytical techniques were used to characterize the Ag nanoparticles:

The biomolecules related to the Au nanoparticles reduction including secondary metabolites were detected by the FT-IR (Shimadzu IR affinity.1). In the UV–Vis spectroscopy analysis, characteristic absorption bands of Au metal were examined before and after the nanoparticles synthesis process. TEM and FE-SEM analysis of the Au nanoparticles was performed with JEOL 200 kV by placing them on a carbon-coated copper grid.

2.3. Investigation of the antioxidant capacity of AuNPs

The DPPH method is a common method for the assessment of the antioxidant activity of plant species and metallic nanoparticles. It is based on trapping the free radicals of the material, called DPPH, using antioxidant agents which reduce the absorption rate at 517 nm wavelength. When the DPPH solution is mixed with a material that can donate hydrogen atom, radical resuscitation is formed, which is followed by color reduction. This reaction eliminates the purple color; whose index is the formation of an absorption band at 517 nm (Hosseinimehr et al., 2011).

To determine the radical scavenging activity of the HAuCl₄, *A. sativum*, and AuNPs, 1 mL of 50 µm DPPH was combined with 1 mL of variable concentrations (0–1000 µg/mL) of HAuCl₄, *A. sativum*, and AuNPs. Then, they were transferred to the 37 °C for 1 h. The samples absorption rate was determined at 517 nm by a spectrophotometer, and the antioxidant activity was calculated by the below formula (Hosseinimehr et al., 2011):

$$\%\text{Inhibiton} = [(A_{blank} - A_{sample})/A_{blank}] \times 100$$

The blank sample contained 1 mL methanol and 1 mL HAuCl₄, *A. sativum*, and AuNPs, and a sample of 1 mL DPPH (Hosseinimehr et al., 2011).

Calculation of half-maximal inhibitory concentration (IC50) is a suitable method for comparison of the activity of pharmaceutical materials. In this method, the measurement and comparison criterion is the concentration in which 50% of the final activity of the drug occurs. In this experiment, the IC50 of various repeats is estimated and compared with the IC50 of BHT, which is introduced as the antioxidant activity index. The closer is the obtained value to the IC50 of BHT, the stronger is the antioxidant activity of the material. The graph of the IC50 of the extract was produced by drawing the percent inhibition curve versus the extract concentration. First, three stock samples with variable concentrations (0–1000 µg/mL) of HAuCl₄, *A. sativum*, and AuNPs were prepared. Then, a serial dilution was prepared from each sample, and IC50 of the above samples was measured separately, following which their mean was calculated. BHT, with different concentrations, was considered positive control. All experiments were performed in triplicate (Hosseinimehr et al., 2011).

2.4. Measurement of cell toxicity of AuNPs

To determine the anti-colon cancer effects of the HAuCl₄, *A. sativum*, and AuNPs, we used following cell lines according to the MTT assay:

(1) HUVEC: Normal cell line.
(2) HT-29: Colorectal adenocarcinoma.
(3) HCT 116: Colorectal carcinoma.
(4) HCT-8 [HRT-18]: Ileocecal colorectal adenocarcinoma.
(5) Ramos.2G6.4C10: Burkitt's lymphoma.

They were then cultured as a monolayer culture in 90% RPMI-1640 medium and 10% fetal serum and supplemented with 200 mg/mL streptomycin, 125 mg/mL penicillin, and 8 mg/mL amphotericin B. The culture was then exposed to 0.5 atmospheric carbon dioxide at 37 °C, on which the tests were performed after at least ten successful passages. MTT assay a method used to investigate the toxic effects of various materials on various cell lines, including non-cancer and cancer cells. To evaluate the cell toxicity effects of the compounds used in this research, the cells were transferred from the T25 flask to the 96-well flasks. In each cell of the 96-cell flasks, 7000 cells of cancer and fibroblast cell lines were cultured, and the volume of each cell was eventually increased to 100 μL. Before the treatment of the cells in the 96-well flak, the density of cells was increased to 70%, so the 96-well flasks were incubated for 24 h to obtain the cell density of 7×10^3. Next, the initial culture medium was discarded, and variable concentrations (0–1000 μg/mL) of HAuCl$_4$, A. sativum, and AuNPs were incubated at 37 °C and 0.5 CO$_2$ for 24, 48, and 72 h. Then, 20 μL MTT was added to each well after a certain amount of time. Next, 100 μL DMSO solvent was added to each well. They were then kept at room temperature for 25 min and read at 490 and 630 nm by a microtitre plate reader (Arulmozhi et al., 2013).

The cell lines were treated with the hydroalcoholic extract (1.25 mg/mL), which inhibited about 20% of the cell growth. Annexin/PI method was used to determine the apoptosis level in the treated and control cell lines using a flow cytometry machine. To perform experiment, the cell lines were treated with a variable concentration (0–1000 μg/mL) of HAuCl$_4$, A. sativum, and AuNPs for 24 h. Cells were irrigated with phosphate-buffered saline (PBS). After centrifugation, buffer binding was added to the obtained precipitate. Then, 5 μL Annexin V dye was added and incubated for 15 min at 25 °C. Cells were washed with the binding solution, following which 10 μL PI dye was added. Finally, cell analysis was done by a flow cytometry machine according to the below formula (Arulmozhi et al., 2013):

$$Cell\ viability(\%) = \frac{Sample\ A.}{Control\ A.} \times 100$$

2.5. Statistical analysis

The obtained results were analyzed by SPSS (version 20) software using one-way ANOVA, followed by Duncan post-hoc test ($P \leq 0.01$).

3. Results and discussion

3.1. UV–visible spectroscopy

At the start of the experiment, immediately the solution light color turned dark yellow, showing the formation of AuNPs, characterized by the UV–Vis spectrum with λmax of around 523 nm. (Fig. 1). Produced AuNPs were collected by centrifugation for analysis in subsequent studies. In the previous studies, the criteria of gold nanoparticles synthesizing were the dark yellow color similar to our studies (Zhaleh et al., 2019; Tahvilian et al., 2019).

Previous studies have indicated that for the biosynthesis of gold oxide, there should also be a peak with at a wavelength range of 510–550 nm (Tahvilian et al., 2019).

Zhaleh et al. (2019) indicated the Gundelia tournefortii L. green-formulated Au nanoparticles have a clear peak at a wavelength of 528 nm. Zangneh et al. assessed Falcaria genus green-synthesized Au nanoparticles with a high peak in the wavelength of 535 nm (Zhaleh et al., 2019).

3.2. FT-IR analysis

In the recent study, FT-IR characterization was carried out on a Thermo Scientific Nicolet iS5 Infrared Spectrometer using the KBr pellet method over the range 400–4000 cm^{-1}.

The analysis of the IR spectrum of the gold nanoparticles revealed the peaks at 514, 1048, 1384–1612, and 3326 cm^{-1} related to the Au-O, C—O, C=C and C=O, and OH, respectively (Fig. 2). The IR spectrum investigated for the gold nanoparticles revealed the absorption peaks at (I) 3287 cm^{-1} (OH group of alcohols and phenols); (II) 1623 cm^{-1} (C=O group of carboxylic acid group); (III) 1383 cm^{-1} (C=C stretching of carboxylic acid group); (IV) 1038 cm^{-1} (C—O vibrations of the protein/polysaccharide) (Hemmati et al., 2019; Varma, 2012).

3.3. FE-SEM and TEM analysis

The image of FE-SEM of gold nanoparticles is revealed in Fig. 3. The gold nanoparticles looked as an agglomerated structure. The OH groups present in A. sativum leaf could be responsible for agglomeration.[22] Also, the image of FE-SEM revealed the average size of 19 nm and the spherical shape for gold nanoparticles. Many similar observations are observed by Shahriari et al., Zhaleh et al. (2019), and Hemmati et al. (2019) (Zhaleh et al., 2019; Hemmati et al., 2019).
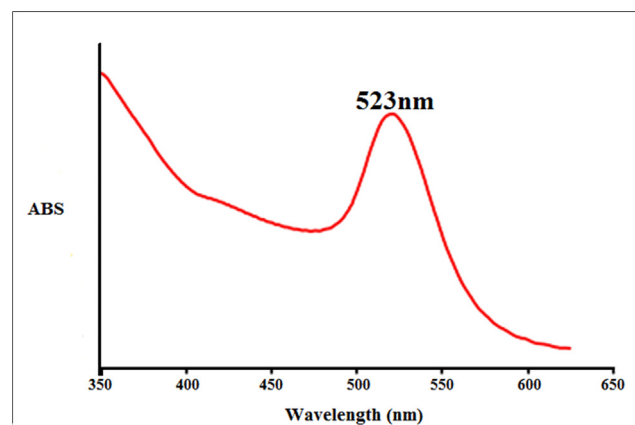
Fig. 1 The UV–Vis spectrum of biosynthesized gold nanoparticles.
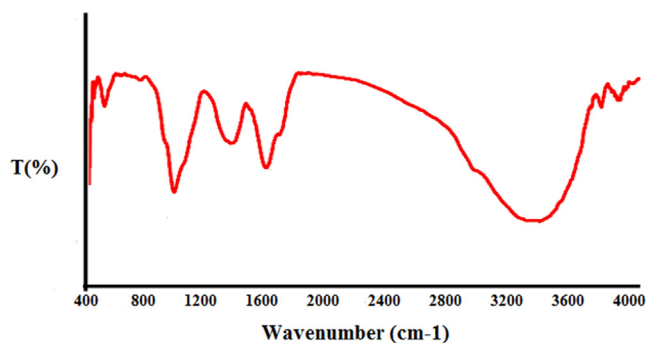
Fig. 2　FT-IR spectrum of biosynthesized gold nanoparticles.
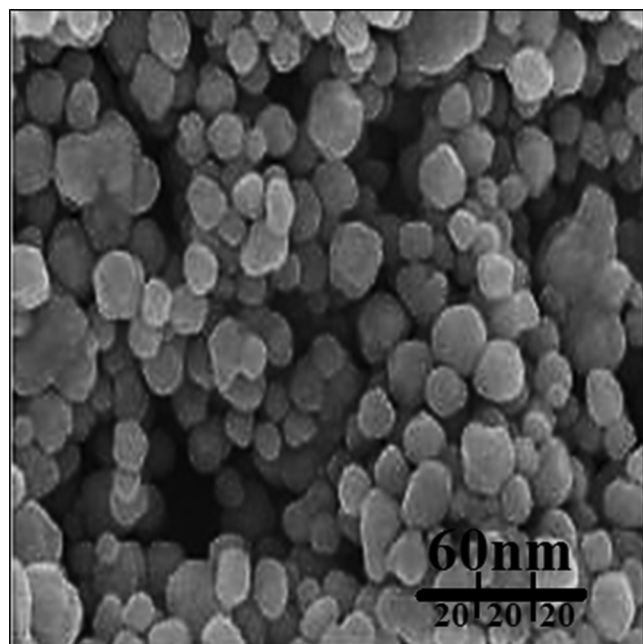
Fig. 3　FE-SEM image of gold nanoparticles.

Fig. 4　TEM image of gold nanoparticles.

Also, the AuNPs average size (19 nm) was determined through images of TEM (Fig. 4). The TEM image histogram plot revealed the bioformulated gold nanoparticles particle size distribution ranges from 7 to 27 nm. The previous researches have reported the ranges of 10–50 nm and spherical shape for biosynthesized of gold nanoparticles (Zhaleh et al., 2019).

3.4. Antioxidant properties of gold nanoparticles against DPPH

Free radicals are molecules that do not have a complete electron shell, which increases the chemical reaction relative to others. Free radicals are formed if you are exposed to tobacco smoke and radiation. In humans, the most important free radical is oxygen. When an oxygen molecule (O_2) is exposed to radiation, it removes an electron from the other molecules, destroying DNA and other molecules. Some of these changes cause disease. Problems such as heart problems, muscle failure, diabetes and cancer are all caused by these free radicals.[23] Antioxidants act like a broom against free radicals, destroying free radicals and regenerating damaged cells. Laboratory evidence has shown that antioxidants can prevent cancer (Singh et al., 2018).
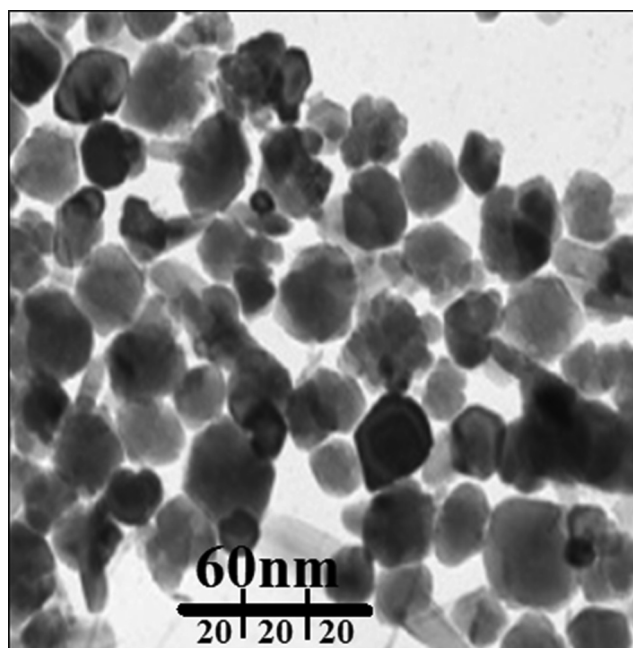
In the current experiment, the DPPH free radical scavenging potential of *A. sativum* leaf aqueous extract and AuNPs in many concentrations revealed impressive prevention similar to BHT. The IC_{50} of *A. sativum* leaf aqueous extract, BHT, and AuNPs were 421, 259, and 231 µg/mL, respectively (Fig. 5; Table 1). Metallic gold nanoparticles also have excellent potential to inhibit DPPH. Following our ingredients, in many studies, the mutual effect has been monitored to increase the antioxidant capacities between herbs and $HAuCl_4$ against DPPH (Singh et al., 2018; Tahvilian et al., 2019).

In general, metal nanoparticles have very extraordinary antioxidant effects, among which the antioxidant effects of gold nanoparticles have been more special. In the recent study, the potent free radical scavenging property of the nanoparticles is noticed at IC_{50} value 231 µg/mL. This may be due to their ability to donate electrons or hydrogen ions to DPPH free radicals to neutralize them. When the concentration is increased, radical scavenging is also increased proportionally. Moreover, the plant contains most of the bioactive compounds which have been attributed to their antioxidant ability (Singh et al., 2018; Tahvilian et al., 2019).

Thomson and Ali (2003) indicated that *A. sativum* is rich of antioxidant compounds such as 3-vinyl-6H-1,3-dithiin, methyl methanesulfinate, dimethyl sulfide, methyl propyl disulfide, S-propyl cysteine sulfoxide, 3-vinyl-6H-1,2-dithiin, dipropyldi sulfide, dimethyl disulfide, 3-vinyl-4H-1,2-dithiin, allyl methyl thiosulfinate, diallyl disulfide, S-methyl cysteine sulfoxide, S-allyl cysteine sulfoxide, allyl methane sulfinate, dipropyl sulfide, dially trisulfide, diallyl tetrasulfide, methyl allyl trisulfide, and diallyl thiosulfinate, and the excellent antioxidant properties of *A. sativum* leaf aqueous extract are related to these compounds (Hosseinimehr et al., 2011). Several studies were carried out in the nanotechnology field using various medicinal
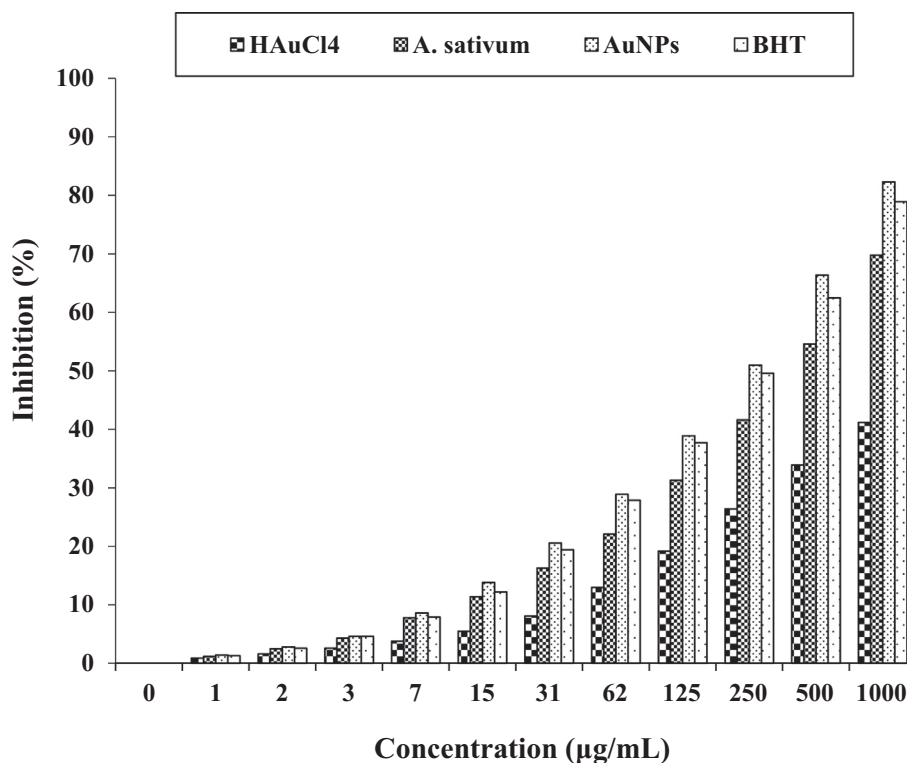
Fig. 5 The antioxidant properties of HAuCl$_4$, *A. sativum*, AuNPs, and BHT against DPPH.

Table 1 The IC$_{50}$ of HAuCl$_4$, *A. sativum*, AuNPs, and BHT in the antioxidant test.

	HAuCl$_4$ (μg/mL)	*A. sativum* (μg/mL)	AuNPs (μg/mL)	BHT (μg/mL)
IC$_{50}$ against DPPH	–	421	231	259

plants, but still, no report is available on gold nanoparticles synthesized using *A. sativum* leaf aqueous extract.

3.5. Cytotoxicity potential of gold nanoparticles

In our study, the treated cells with several concentrations of the present HAuCl$_4$, *A. sativum*, and AuNPs were examined by MTT test for 48 h regarding the cytotoxicity properties on normal (HUVEC), colorectal adenocarcinoma (HT-29), colorectal carcinoma (HCT 116), ileocecal colorectal adeno-carcinoma (HCT-8 [HRT-18]), and Burkitt's lymphoma (Ramos.2G6.4C10) cell lines (Figs. 6-10; Table 2). The absor-bance rate was determined at 570 nm, which indicated extraor-dinary viability on normal cell line (HUVEC) even up to 1000 μg/mL for HAuCl$_4$, *A. sativum*, and AuNPs.

In the case of colon cancer cell lines, the viability of them decreased dose-dependently in the presence of gold salt, *A. sativum*, and AuNPs. The IC50 of *A. sativum* and AuNPs against HT-29 cell line were 417 and 269 μg/mL, respectively; against Human HCT 116 cell line were 361 and 225 μg/mL, respectively; against HCT-8 [HRT-18] cell line was 402 and 250 μg/mL, respectively; and against Ramos.2G6.4C10 cell line were 380 and 236 μg/mL, respectively. The best result of

cytotoxicity property of gold nanoparticles against the above cell lines was seen in the case of the HCT 116 cell line.

In the present study, the cytotoxicity of the gold nanopar-ticles on the normal cell line, HUVEC, was weaker than those on the colon cancer cell lines. The reason of the resent phe-nomenon is related to the cancer cell structure (Arulmozhi et al., 2013; Ramyadevi et al., 2012; Reuter et al., 2010). The cancer cell is characterized by: acceleration of the cell cycle; genomic alterations; invasive growth; increased cell mobility; chemotaxis; changes in the cellular surface; secretion of lytic factors, etc (Gultekin et al., 2016; Rehana et al., 2017). Mor-phological and functional characteristics of the malignant cell. Morphologically, the cancerous cell is characterized by a large nucleus, having an irregular size and shape, the nucleoli are prominent, the cytoplasm is scarce and intensely colored or, on the contrary, is pale (Del Mar Delgado-Povedano et al., 2016). The *nucleus* of neoplastic cells plays through its changes a main role in the assessment of tumor malignancy. Changes concern its surface, volume, the nucleus/cytoplasm ratio, shape and density, as well as structure and homogeneity (Jeong et al., 2012; Sankar et al., 2014). Ultrastructural characteristics are related to nucleus segmentation, invaginations, changes in chromatin, such as heterochromatin reduction, increase of
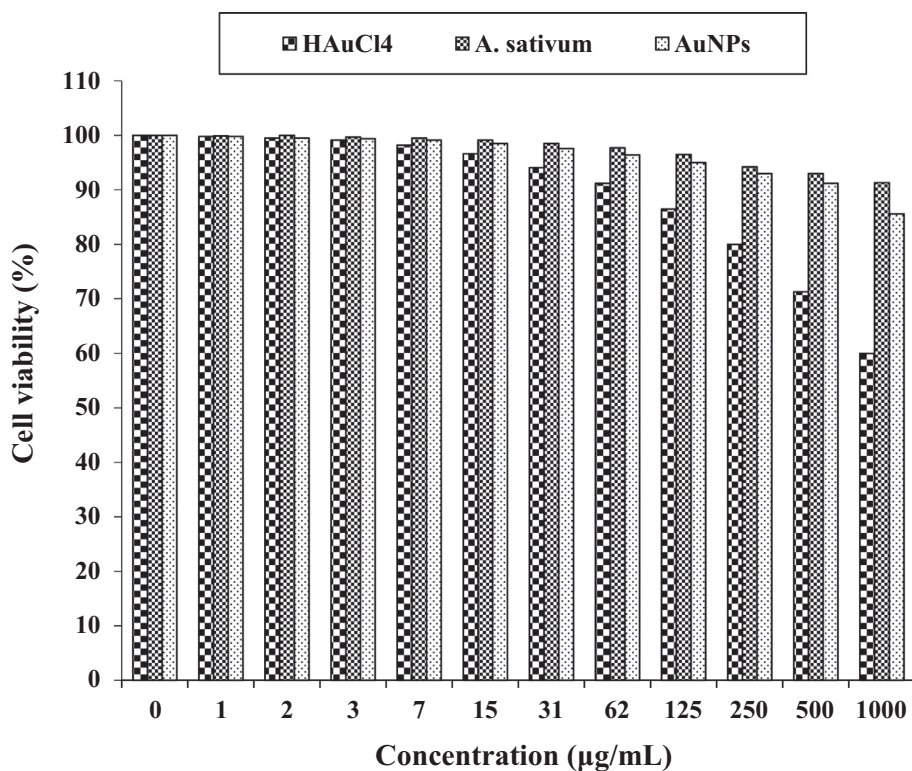
Fig. 6   The cytotoxicity properties of HAuCl₄, *A. sativum*, and AuNPs against HUVEC cell line.
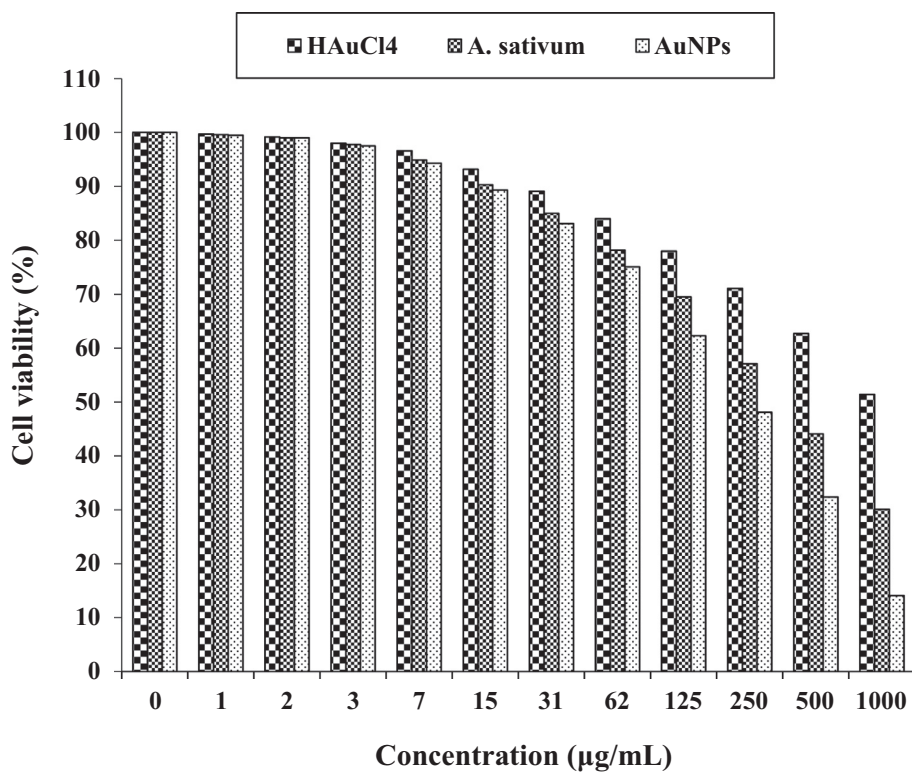
Fig. 7   The anti-colorectal adenocarcinoma properties of HAuCl₄, *A. sativum*, and AuNPs against HT-29 cell line.

interchromatin and perichromatin granules, increase of nuclear membrane pores, formation of inclusions, etc. The nucleolus is characterized by hypertrophy, macro- and microsegregation, its movement towards the membrane, numerical increase and formation of intranuclear canalicular systems between the nuclear membrane and the nucleolus
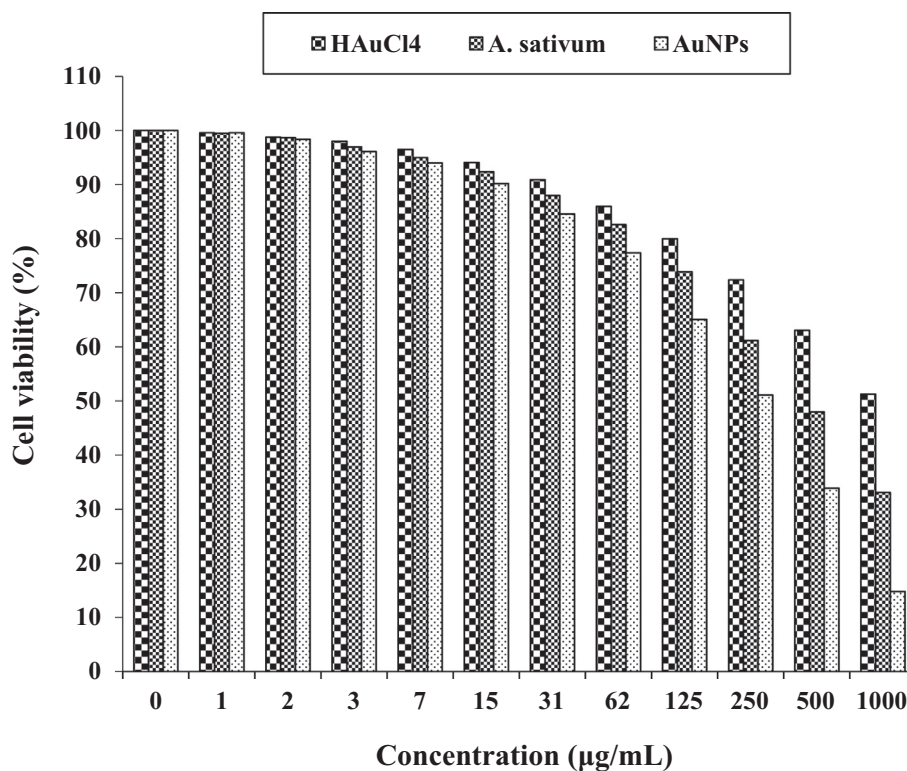
Fig. 8   The anti-colorectal carcinoma properties of HAuCl$_4$, *A. sativum*, and AuNPs against HCT 116 cell line.
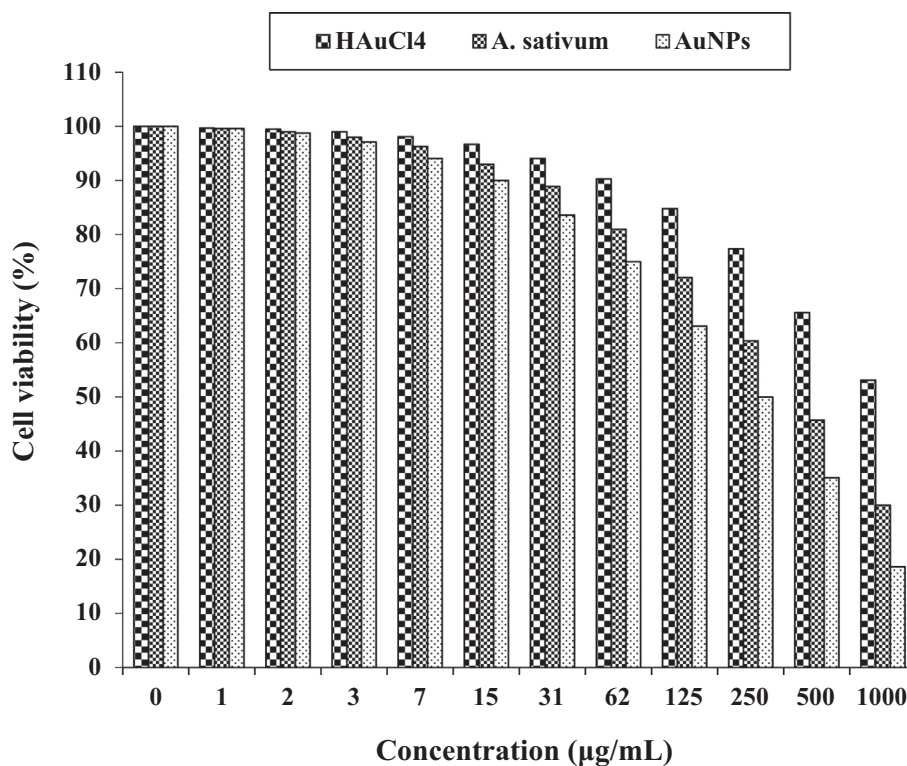
Fig. 9   The anti-ileocecal colorectal adenocarcinoma properties of HAuCl$_4$, *A. sativum*, and AuNPs against HCT-8 [HRT-18] cell line.

(Namvar et al., 2014). Mitoses are characteristic of malignant cells. The number of mitoses increases, atypical mitosis forms with defects in the mitotic spindle appear, which results in tri-

ple or quadruple asters and dissymmetrical structures and atypical forms of chromosomes. Nuclear changes explain the presence of different cell clones and genetic anomalies associ-
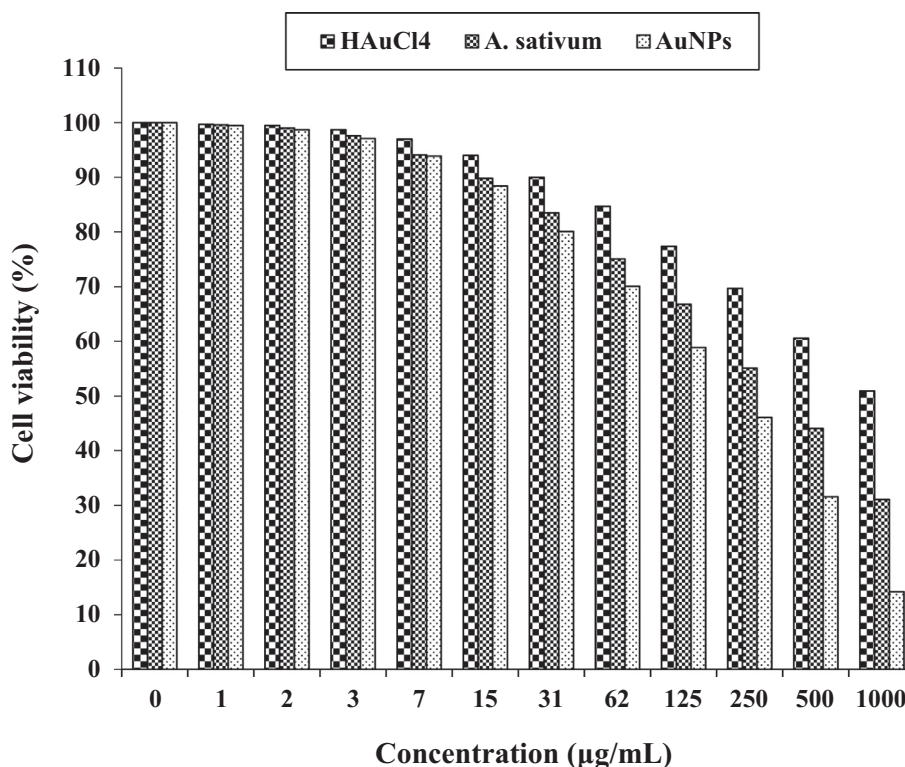
Fig. 10 The anti-Burkitt's lymphoma properties of HAuCl4, *A. sativum*, and AuNPs against Ramos.2G6.4C10 cell line.

Table 2 The IC$_{50}$ of HAuCl$_4$, *A. sativum*, and AuNPs in the cytotoxicity test.

	HAuCl$_4$ (μg/mL)	*A. sativum* (μg/mL)	AuNPs (μg/mL)
IC$_{50}$ against HUVEC	–	–	–
IC$_{50}$ against HT-29	–	417	269
IC$_{50}$ against HCT 116	–	361	225
IC$_{50}$ against HCT-8 [HRT-18]	–	402	250
IC$_{50}$ against Ramos.2G6.4C10	–	380	236

ated with these changes. In intensely anaplastic tumors, the presence of gigantic nuclei and multinucleate cells expresses abnormal divisions. These morphological characteristics reflect the changes occurring at metabolic level, with the augmentation of structures in relation to cell division and the attenuation of structures associated to other metabolisms (Katata-Seru et al., 2018; Sangami and Manu, 2017). The above reasons are caused that the cytotoxicity of the gold nanoparticles on HUVEC was weaker than those on the colon cancer cell lines.

Among the various agents of metallic nanoparticles such as, surface functions nature, texture, size, and morphology, the size efficacy is most necessary in the anticancer test. Previous researches indicated that the anticancer property enhances with reducing in size of particle based on their better penetration property over the cell lines. It has been determined that the size of particle lower than 50 nm demonstrates better effect in the corresponding cancer cell lines (Namvar et al., 2014). As can be observed in Figs. 4 and 5 of the recent study, the sizes of Au nanoparticles synthesized by *A. sativum* leaf aqueous extract are at the ranges of 7–27 nm.

About the anticancer capacities of Au nanoparticles, they have applied to cure various cancers including human glioma, Lewis lung carcinoma, uterus cancer, human lung cancer, colon cancer, lung epithelial cancer, and mammary carcinoma (Katata-Seru et al., 2018).

Likely the significant anti-colon cancer potentials of gold nanoparticles synthesized by *A. sativum* aqueous extract against colon cancer cell lines are linked to their antioxidant activities. Similar researches have revealed the antioxidant materials such as metallic nanoparticles especially gold nanoparticles and ethnomedicinal plants reduce the volume of tumors by removing free radicals (Sangami and Manu, 2017). In detail, the high presence of free radicals in the normal cells makes many mutations in their DNA and RNA, destroys their gene expression, and then accelerates the proliferation and growth of abnormal cells or cancerous cells. The free radicals high presences in all cancers such as skin, throat, ovarian, testicular, bladder, colon, small intestine, gastrointestinal stromal, stomach, breast, lung, vaginal, prostate, pancreatic, liver, gallbladder, hypopharyngeal, fallopian tube, thyroid, esophageal, parathyroid, bile duct, and rectal cancers indicate the significant role of these molecules in making angiogenesis and tumorigenesis (Beheshtkhoo et al., 2018; Radini et al., 2018). Many researchers reported that gold nanoparticles synthesized by ethnomedicinal plants with high antioxidant compounds have a remarkable role in removing free radicals and growth inhibition of all cancerous cells (Oganesvan et al., 1991).

4. Conclusion

In this research, the Au nanoparticles were attained from the reaction between $HAuCl_4$ and *A. sativum* leaf aqueous extract in vitro condition. TEM, FE-SEM, UV–Vis, and FT-IR methods were utilized to evaluate nanoparticle characteristics. The results of these techniques revealed that Au nanoparticles had been synthesized in the best way. Base on the FT-IR spectrum the presence of a great number of antioxidant compounds produced appropriate conditions for the reduction of gold. In the TEM technique, the mean size of Au nanoparticles was assessed to be 19 nm, which is favorable.

The Au nanoparticles showed the best antioxidant activities against DPPH. Au nanoparticles had appropriate anti-colon cancer activities dose-dependently against HT-29, HCT 116, HCT-8 [HRT-18], and Ramos.2G6.4C10 cell lines without any cytotoxicity on the normal cell line (HUVEC). After clinical study Au nanoparticles containing *A. sativum* leaf aqueous extract can be utilized as an efficient drug in the treatment of colon cancer and diseases in humans.

Declaration of Competing Interest

The authors declare that they have no known competing financial interests or personal relationships that could have appeared to influence the work reported in this paper.

Acknowledgement

References

Ahmeda, A., Zangeneh, A., Zangeneh, M.M., 2020. Appl. Organometal. Chem. 34,. https://doi.org/10.1002/aoc.5290 e5290.

Arulmozhi, V., Pandian, K., Mirunalini, S., 2013. Colloids Surf B Biointerfaces. 110, 313–320.

Arunachalam, K.D., Annamalai, S.K., Hari, S., 2003. Int. J. Nanomed. 8, 1307–1315.

Astin, M., Griffin, T., Neal, R.D., Rose, P., Hamilton, W., 2011. Br. J. Gen. Pract. 61, 231–243.

Ball, V., 2018. Front. Bioeng. Biotechnol. 6, 109.

Beheshtkhoo, N., Kouhbanani, M.A.J., Savardashtaki, A., Amani, A. M., Taghizadeh, S., 2018. Appl. Phys. A 124, 363–369.

Cunningham, D., Atkin, W., Lenz, H.J., Lynch, H.T., Minsky, B., Nordlinger, B., Starling, N., 2010. Lancet 375, 1030–1047.

Del Mar Delgado-Povedano, M., Medina, V.S.D., Bautista, J., Priego-Capote, F., De, M.D., Castro, M.D., 2016. J. Function Foods 24, 403–419.

Ghaneialvar, H., Sahebghadam Lotfi, A., Arjmand, S., et al, 2019. Comp. Clin. Path. 28, 1077–1085.

Goorani, S., Koohi, M.K., Zangeneh, A., et al, 2019. Comp. Cli. Path 28 (5), 1221–1227.

Goorani, S., Koohi, M.K., Morovvati, H., Hassan, J., Ahmeda, A., Zangeneh, M.M., 2020. Appl. Organometal. Chem. 34, e5465.

Gultekin, D.D., Gungor, A.A., Onem, H., Babagil, A., Nadaroglu, H., 2016. J. Turk. Chem. Soc. A: Chem. 3, 623–636.

Hemmati, S., Joshani, Z., Zangeneh, A., Zangeneh, M.M., 2019. Appl. Organometal. Chem. 33,. https://doi.org/10.1002/aoc.5267 e5267.

Hosseinimehr, S.J., Mahmoudzadeh, A., Ahmadi, A., Ashrafi, S.A., Shafaghati, N., Hedayati, N., 2011. Cancer Biother. Radiopharm. 26, 325–329.

Jalalvand, A.R., Zhaleh, M., Goorani, S., et al, 2019. J. Photochem. Photobiol., B 192, 103–112.

Jeong, S.C., Koyyalamudi, S.R., Jeong, Y.T., Song, C.H., Pang, G., 2012. J. Med. Food 1, 58–65.

Juul, J.S., Hornung, N., Andersen, B., Laurberg, S., Olesen, F., Vedsted, P., 2018. Br. J. Cancer 119, 471–479.

Katata-Seru, L., Moremedi, T., Aremu, O.S., Bahadur, I., 2018. J. Mol. Liq. 256, 296–304.

Lauby-Secretan, B., Scoccianti, C., Loomis, D., Grosse, Y., Bianchini, F., Straif, K., 2016. N. Engl. J. Med. 375, 794–798.

Mahdavi, B., Paydarfard, S., Zangeneh, M.M., Goorani, S., Seydi, N., Zangeneh, A., 2019. Appl. Organometal. Chem. 33,. https://doi.org/10.1002/aoc.5248 e5248.

Mohammadi, G., Zangeneh, M.M., Zangeneh, A., Siavosh Haghighi, Z.M., 2019. Appl. Organometal. Chem. 33,. https://doi.org/10.1002/aoc.5136 e5136.

Moradi, R., Hajialiani, M., Salmani, S., et al, 2019. Comp. Cli. Path. 28 (5), 1205–1211.

Namvar, F., Rahman, H.S., Mohamad, R., Baharara, J., Mahdavi, M., Amini, E., Chartrand, M.S., Yeap, S.K., 2014. Int. J. Nanomed. 19, 2479–2488.

Oganesvan, G., Galstyan, A., Mnatsakanyan, V., Paronikyan, R., Ter-Zakharyan, Y.Z., 1991. Chem. Nat. 27, 247.

Radini, I.A., Hasan, N., Malik, M.A., Khan, Z., 2018. J. Photochem. Photobiol., B 183, 154–163.

Ramyadevi, J., Jeyasubramanian, K., Marikani, A., Rajakumar, G., Rahuman, A.A., 2012. Mater. Lett. 71, 114.

Rashidi, K., Mahmoudi, M., Mohammadi, G., et al, 2018. Int. J. Biol. Macromol. 120, 587–595.

Raut, R.W., Kolekar, N.S., Lakkakula, J.R., Mendhulkar, V.D., Kashid, S.B., 2010. Nano-Micro Lett. 2, 106.

Rehana, D., Mahendiran, D., Kumar, R.S., Rahiman, A.K., 2017. Biomed. Pharmacother. 89, 1067–1077.

Reuter, S., Gupta, S.C., Chaturvedi, M.M., Aggarwal, B.B., 2010. Biol. Med. 11, 1603–1616.

Sangami, S., Manu, B., 2017. Environ. Technol. Innov. 8, 150–163.

Sankar, R., Maheswari, R., Karthik, S., Shivashangari, K.S., Ravikumar, V., 2014. Mat. Sci. Eng. C. 44, 234–239.

Shaib, W., Mahajan, R., El-Rayes, B., 2013. J. Gastrointest. Oncol. 4, 308–318.

Sherkatolabbasieh, H., Hagh-Nazari, L., Shafiezadeh, S., Goodarzi, N., Zangeneh, M.M., Zangeneh, A., 2017. Arch. Biol. Sci. 69 (3), 535–543.

Singh, P., Pandit, S., Mokkapati, V.R.S.S., Garg, A., Ravikumar, V., Mijakovic, I., 2018. Int. J. Mol. Sci. 10, 1979.

Sintubin, L., Windt, W.D., Dick, J., Mast, J., van der Ha, D., Verstraete, W., Boon, N., 2009. Appl. Microbiol. Biotechnol. 6, 741–749.

Soni, A., Krishnamurthy, R., 2013. Indian J. Plant Sci. 2, 117–125.

Tahvilian, R., Zangeneh, M.M., Falahi, H., et al, 2019. Appl. Organometal. Chem. 33,. https://doi.org/10.1002/aoc.5234 e5234.

Thomson, M., Ali, M., 2003. Curr. Cancer Drug Targets 3, 67–81.

Varma, R.S., 2012. Curr. Opin. Chem. Eng. 1, 123.

Zangeneh, M.M., 2019. Appl. Organometal. Chem. 33,. https://doi.org/10.1002/aoc.5295 e5295.

Zangeneh, A., Zangeneh, M.M., Moradi, R., 2019. Appl. Organometal. Chem. 33,. https://doi.org/10.1002/aoc.5247 e5247.

Zangeneh, A., Zangeneh, M.M., 2019. Appl. Organometal. Chem. 33. https://doi.org/10.1002/aoc.5290.

Zhaleh, M., Sohrabi, N., Zangeneh, M.M., et al, 2018. J. Essent. Oil Bear Pl. 21 (2), 493–501.

Zhaleh, M., Zangeneh, A., Goorani, S., et al, 2019. Appl. Organometal. Chem. 33,. https://doi.org/10.1002/aoc.5015 e5015.